



Toughening improvement to a soybean meal-based bioadhesive using an interpenetrating acrylic emulsion network

Jianlin Luo¹, Jing Luo¹, Xiaona Li¹, Kun Li¹, Qiang Gao^{1,*}, and Jianzhang Li^{1,*}

¹MOE Key Laboratory of Wooden Material Science and Application, Beijing Key Laboratory of Lignocellulosic Chemistry, MOE Engineering Research Centre of Forestry Biomass Materials and Bioenergy, Beijing Forestry University, Beijing 100083, China

Received: 16 May 2016

Accepted: 25 June 2016

Published online:

11 July 2016

© Springer Science+Business Media New York 2016

ABSTRACT

The goal of this investigation was to improve the water resistance of soybean meal-based (SM) bioadhesive and enhance the mechanical properties of the bonded plywood by combining triglycidylamine (TGA) cross-linking with an acrylic emulsion interpenetrating network (IPN). The solid content, functional groups, crystallinity, mass loss after hydrolyzing, fracture surface micrographs, and thermal stability of the resulting adhesives were characterized. Three-ply plywood was fabricated and its dry and wet shear strength was determined. The experimental results indicated that the introduction of 8 % TGA produced an improvement of 15.1 % in the water resistance of SM adhesive and 86.8 % in the wet shear strength of plywood as a result of the chemical cross-linking between epoxy groups and protein molecules. However, this reaction increased the brittleness of adhesive and caused an insufficient dry bond strength. Incorporating 8 % AE into the SM/TGA adhesive resulted in a water resistance that was improved by 24.6 %, a dry shear strength that was increased by 44.0 % to 1.80 MPa and a wet shear strength that was increased by 47.9 % to 1.05 MPa. The improvements were attributed to the formation of IPN which increased the solid content, improved the toughness of the adhesive, and promoted an uniform and compact cured structure. All results suggested that chemical cross-linking can effectively improve the water resistance of SM adhesive, but will aggravate the brittleness. Toughening improvement is an effective approach to enhance the performance of the SPAs and solve the low dry strength issue of resulting composites.

Address correspondence to E-mail: gaoqiang@bjfu.edu.cn; lijzh@bjfu.edu.cn

Introduction

Until recently, formaldehyde-based synthetic resins, such as urea, melamine, and phenol–formaldehyde resins still dominate the bonding of wood composites, primarily because of their attractive advantages including low cost, initial water solubility, fast cure rate, and excellent adhesion to wood. However, these synthetic adhesives are nonrenewable and have environmental pollution and nonsustainable issues. Consequently, eco-friendly bioadhesives derived from renewable materials have been widely investigated in recent years [1].

Biomass resources, including tannins, lignins, carbohydrates, unsaturated oils, and protein, are potential renewable sources for the development of bioadhesives [2, 3]. Proteins, especially vegetable proteins, are renewable and eco-friendly biopolymers. However, more than one-third of protein sources are underutilized and could be used as raw materials for new protein-based industrial products [4]. A variety of vegetable proteins have been used to develop bioadhesives, such as cottonseed protein [5], wheat gluten [6], sorghum protein [7], peanut protein [8], and soy protein [9]. The high volume availability and low cost of soybean make soy protein-based adhesives (SPAs) the most promising alternative to formaldehyde-based synthetic products [10].

The utilization of SPAs dates back to the 1920s when almost all interior plywood in America was fabricated using this adhesive [11]. Subsequently, the market was dominated by petrochemical-based synthetic adhesives, because of their ease of use, high curing condition adaptability, and improved water resistance. Although research on SPAs has been revived in recent years, the low water resistance of this adhesive still greatly limits the application. Many modification methods have been made to tackle this limitation. One method focused on using the protein denaturing agent. The hydrophobic interaction of the soybean protein molecule leads to protein folding and the formation of a hydrophobic cluster. Researchers have employed alkali [12], urea [13], and sodium dodecyl sulfate [14] to denature the soy protein molecule and turn it inside out for exposing the buried hydrophobic groups, which improved the water resistance of adhesive by promoting protein–protein interaction. However, this effect of protein modification is limited and cannot meet the interior plywood requirements, because the hydrophilic groups in the protein are also

exposed. Another method was cross-linking modification. Glutaraldehyde [15], maleic anhydride [16], and polyethylene glycol diacrylate [17] were adopted as a mean of cross-linking the soy protein. These cross-linkers reacted with the active groups in the protein molecules, transforming weak intermolecular interactions into stable chemical bonds, which elevated the adhesive performance. In our previous studies, soybean meal was blended with glycerol polyglycidyl ether [18], ethylene glycol diglycidyl ether [19], and 5,5-dimethyl hydantoin polyepoxide [20] to prepare soybean meal-based (SM) wood adhesives with significantly improved water resistance. It was found that a resin or an ether which contained at least two active epoxy groups can be an effective cross-linker for the SPAs.

Soy protein is a high molecular weight macromolecular biopolymer. Intermolecular interaction occurs through weak bonds such as hydrogen bonds, electrostatic bonds, van der Waals forces, and disulfide bonds. Therefore, native SPAs exhibit low bond strength, poor water resistance, and high brittleness. After cross-linked by epoxies, the SPAs produced more brittleness and poor resistance to crack propagation, resulting in low mechanical properties. This was especially true in the engineered wood flooring fabrication, which is unacceptable for wood composite industry. Therefore, increasing the toughness of the adhesive system will benefit both its water resistance and mechanical properties of resultant products.

Acrylic emulsion (AE) is an emulsion polymerization product of acrylic/methacrylic acid and vinyl ester monomers [21]. It is widely used in the packaging, coating, spinning, building, and leather industries, because of its unique properties such as low cost, superior adhesion capability, excellent flexibility, and film forming property. Therefore, we believed that the combination of a flexible AE and rigid SPAs might provide superior mechanical properties for the adhesives used for bonded wood products. Moreover, AE possesses a high solid content, low viscosity, and is water based. Therefore, AE could be a potential modifier for improving the toughness and water resistance of SPAs.

In this study, a laboratory-synthesized cross-linker, triglycidylamine (TGA), was combined with a commercial AE to develop a high performance soybean meal-based bioadhesive. The effects of AE on the performance of adhesive and resultant plywood were investigated. Three-ply plywood was fabricated

using the modified adhesive and was tested to determine the dry/wet shear strength. The solid content, functional groups, crystallinity, mass loss after hydrolyzing, fracture surface micrographs, and thermal stability of the resulting adhesives were evaluated to better comprehend the toughening effect of AE on the SPAs system.

Experimental

Materials

Soybean meal (43–48 % soy protein, 30–34 % polysaccharide, 8–10 % moisture, 3–5 % fiber, 5–7 % ash, and 0.2–0.8 % fat) was supplied by Xiangchi Grain and Oil Co., Ltd. (Shandong, China). Commercial acrylic emulsion with a solid content of 46 %, a pH value of 7–9, and a viscosity of 2000 mPa s was provided by Xinyi Chemical Co., Ltd. (Guangdong, China). Analytical grade epichlorohydrin (99 %) and aqueous ammonia (25 %) were purchased from Lanyi Chemical Co., Ltd. (Beijing, China). The poplar veneer with a moisture content of 8.0 % and dimensions of 400 × 400 × 1.5 mm were obtained from a local plywood plant. Other chemical reactants were analytical grade and obtained from Beijing Chemical Reagents Co. Ltd. (China).

Preparation of cross-linker TGA

TGA was synthesized according to a previous report [22], and the reaction pathway was illustrated in Fig. 1. Epichlorohydrin and aqueous ammonia with a mole ratio 5:1 were placed in a three-necked flask equipped with a condenser and stirrer. The mixture was stirred continuously with a rate of 800 rpm. Ammonium triflate was used to catalyze the reaction at 23 °C for 48 h, then 35 °C for 3 h. The residual

epichlorohydrin and ammonium hydroxide were removed by a vacuum distillation process, and the result was a colorless syrup consisting mostly of tris(3-chloro-2-hydroxypropyl)amine (Fig. 1a). An excess of sodium hydroxide solution (50 %) was added for the epoxy-ring closure reaction at 20 °C for 2 h. Because the reaction was highly exo-thermal, an external ice-water cooling circulator was required to hold the temperature. The precipitate of sodium chloride was filtered off, and the residue was vacuum distilled to obtain pure viscous TGA (Fig. 1b).

Preparation of adhesive

In this study, soy protein is provided by soybean meal. SM adhesive was prepared by adding SM (28 g) into water (72 g) and stirring for 10 min at room temperature to form a homogeneous system. Cross-linker TGA (8 % based on the mass of liquid SM adhesive) was added into the SM adhesive and stirred for 10 min to develop the TGA-modified soybean meal (SM/TGA) adhesive. Different amounts of AE (2, 4, 6, 8, 10 % based on the mass of liquid SM adhesive) were incorporated into the SM/TGA adhesive and stirred for 10 min to prepare the AE-modified SM/TGA (SM/TGA/AE) adhesives.

Solid content of adhesive measurement

The solid content of adhesive was measured based on an oven dry method according to the China National Standard GB/T 14074 (2006) [23]. About 3 g adhesive was placed into an oven at a temperature of 105 ± 2 °C for drying until a constant weight was obtained. The solid content was calculated (three replications) by weighing the difference of weight before and after drying.

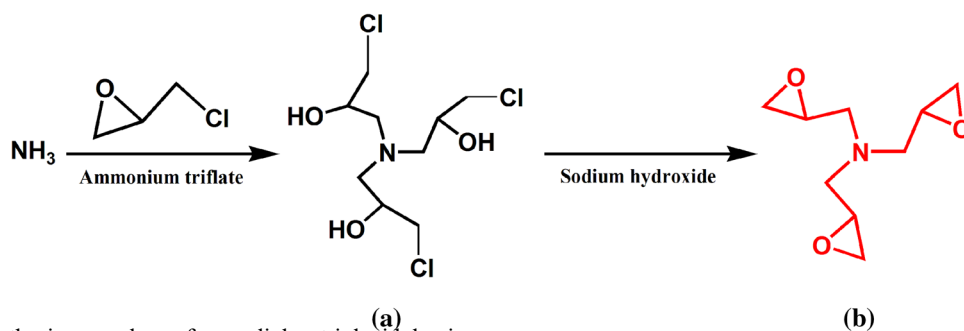


Figure 1 The synthesis procedure of cross-linker triglycidylamine.

Mass loss of cured adhesive after hydrolyzing

An adhesive sample was placed in an oven at 120 ± 2 °C until a constant weight was obtained, and then ground into 100 mesh powder (0.15 mm) by a ceramic mortar. To determine the mass loss, the cured adhesive (three replications) was wrapped up using a qualitative filter paper and placed in a glass with distilled water. After hydrolyzing for 6 h in an oven of 60 ± 2 °C, the sample was dried (105 ± 2 °C, 3 h) and weighed. The mass loss was determined by weighing the difference of weight before and after hydrolyzing.

Preparation of plywood and evaluation

Three-ply poplar plywood was fabricated in this study. Adhesives were evenly coated on both sides of the core veneer with a glue spreading of 200 g/m^2 . The coated veneer was stacked between two uncoated veneers with the grain direction of the two adjacent veneers perpendicular to each other. The stacked veneers were hot-pressed at 120 °C and 1.0 MPa for 6 min. Two plywoods were fabricated for the same adhesive formula.

The shear strength of plywood was determined according to the China National Standard GB/T 17657 (2013) [24]. After prepared plywood was equilibrated for at least 24 h under room condition, twelve specimens with dimension of $100 \times 25 \text{ mm}$ (glue area of $25 \times 25 \text{ mm}$) were equably cut from the center and edge of the two plywoods. The schematic diagram of the sample preparation and the force loading is shown in Fig. 2.

The dry shear strength was determined using a common tensile machine operating at a speed of 10.0 mm/min . The force required to break the glued specimen was recorded. The shear strength was calculated according to Eq. (1). The specimens for wet shear strength measurement were immersed in water at 63 ± 3 °C for 3 h, and then dried at room temperature for 10 min before a tension test under the

same testing condition. The reported shear strength was an average value of twelve specimens and the standard deviation was given.

$$\text{Dry/wet shear strength} = \frac{\text{Force (N)}}{\text{Gluing area (m}^2\text{)}}. \quad (1)$$

Fourier transform infrared (FTIR) spectroscopy

Ground cured adhesive powder samples with 200 mesh (0.075 mm) was mixed with KBr crystals at a mass ratio of 1/70, and pressed in a special mold to form a sample folium. The FTIR spectra were recorded using a Thermo Nicolet 6700 FTIR (USA) over the range of $400\text{--}4000 \text{ cm}^{-1}$ with a 4 cm^{-1} resolution and 32 scans.

X-ray diffraction (XRD)

Ground cured adhesive powder samples with 200 mesh (0.075 mm) were analyzed at ambient temperature by an XRD diffractometer (D8 ADVANCE, BRUKER, German) using a Cu K α X-ray source with a wavelength (λ) of 1.5405 \AA , in the 2θ scan ranging from 5° to 60° . The crystallinity of resin sample was calculated by the software of DIFFRAC.EVA V 3.1 (BRUKER, German) based on the area method as Eq. (2) [25].

$$\% \text{ Crystallinity} = \frac{A_{\text{cryst}}}{A_{\text{total}}} \times 100 \%, \quad (2)$$

where A_{cryst} is the sum of crystalline band areas, and A_{total} is the total area under the diffraction patterns. Each adhesive sample was tested three times and the average value was reported.

Toughness evaluation of cured adhesive

For visually evaluating the toughness of cured adhesive, the modified liquid adhesive was uniformly coated on glass slides, and then placed in an oven at a temperature of 120 ± 2 °C for 2 h. After adhesive curing, the coated glass slides were placed

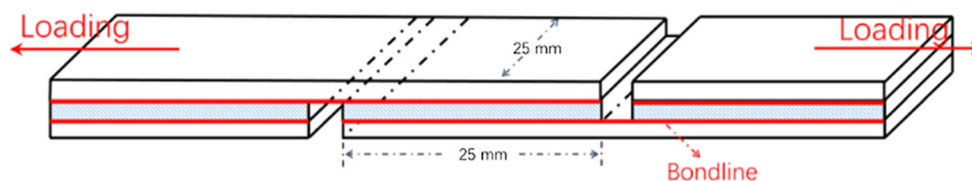


Figure 2 The schematic diagram of the sample preparation and the force loading.

in a desiccator for 30 min. The cooled glass slides were photographed using a Digital Single Lens Reflex.

Scanning electron microscopy (SEM)

For observing the interior microstructure, the fracture surface of cured adhesive was analyzed using SEM. The adhesive samples were completely cured in an oven at 120 ± 2 °C. Then, the samples were placed into a desiccator for 2 days before being examined. The cured adhesives were artificially fractured, and the fracture surfaces were tested. Before testing, the fracture surfaces were placed on an aluminum stub, and a 10-nm gold film was coated on using an ion sputter (HITACHI MC1000, Japan). The coated fracture surfaces were imaged by a JSM-6500F field emission scanning electron microscope (FE-SEM) (JEOL, Japan).

Thermal stability measurement

AE, TGA, AE/TGA, and their modified adhesives were cured completely in an oven at 120 ± 2 °C. The thermal degradation behavior of the cured samples was tested using a TGA instrument (TA Q50, WATERS Company, USA). About 8 mg of powdered adhesive sample with 200 mesh (0.075 mm) was weighed in a platinum cup and scanned from room temperature to 600 °C at a heating rate of 10 °C/min in a nitrogen environment while recording the weight change.

Results and discussion

Solid content of adhesive

The physical and chemical characteristics of both the wood substrate and the adhesive influence the resulting wood-adhesive bonding [26]. The solid content of adhesive is an essential physical parameter that greatly influences the performance of bonded products. A low solid content will allow significant water combination with the coated veneers, which will form a high moisture content slab. As a result, a large quantity of water needs to be removed during hot-pressing process, leading to unstable properties of the bonded plywood and lower product efficiency. In addition, the water evaporation from the inside of

adhesive will cause the cohesive failure of cured adhesive system and impact the water resistance of adhesive. Because of the high molecular weight, molecular entanglement and friction, soy protein has high viscosity but low solid content when it is dissolved in water. Introducing additive into the adhesive rather than adding more soy protein to increase the solid component is necessary and practical for ensuring the flowability of adhesive. The solid content of neat and modified SM adhesive is shown in Fig. 3.

As shown in this figure, neat SM adhesive exhibited the lowest solid content of 27.27 %, which could not obtain an effective bond with the wood substrate. The solid content was increased to 30.44 % by adding 8 % TGA thanks to its high solid content. After the introduction of AE, the solid content gradually increased from 30.44 to 36.38 % as the AE content increased from 2 to 10 %, because adding AE was equivalent to increasing the mass of the adhesive. Previous research has suggested that the solid content of SPAs should be more than 35 % to ensure favorable bond strength [27]. When the AE content was 8 %, the solid content of the adhesive increased by 18 % compared with the SM/TGA adhesive to 35.92 % and met the necessary requirement. The increased solid content is beneficial to the improvement of water resistance of cured adhesive by decreasing the water evaporation. Moreover, the less water evaporation will delay the cohesive failure of cured adhesive during hot-pressing process.

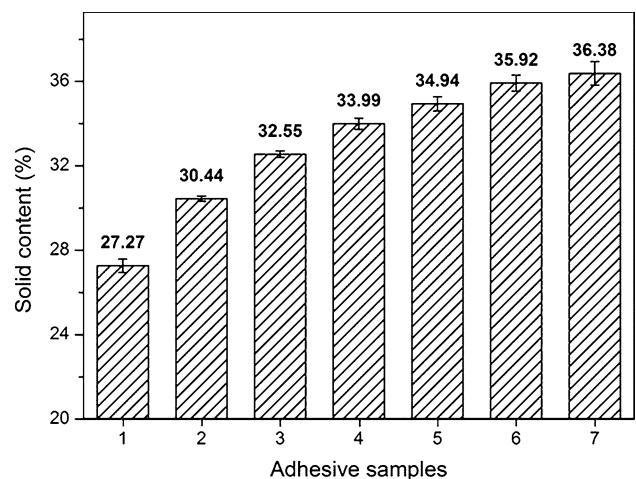


Figure 3 The solid content of adhesive 1 (SM), 2 (SM/TGA), 3 (SM/TGA/2 % AE), 4 (SM/TGA/4 % AE), 5 (SM/TGA/6 % AE), 6 (SM/TGA/8 % AE), 7 (SM/TGA/10 % AE).

FTIR spectroscopic analysis

Figure 4 displays the ATR-FTIR spectra of the AE, TGA, AE/TGA, and the FTIR spectra of the resulting adhesives. The characteristic peaks in AE are present including the $-\text{CH}_3$ absorption peak, $\text{C}=\text{O}$ stretching vibration, $-\text{COO}$ stretching vibration, $\text{C}-\text{O}-\text{C}$ absorption peak, and $\text{C}-\text{H}$ in-plane bending vibration, which appeared at 2955, 1727, 1452, and 1157 cm^{-1} , respectively [21]. In the TGA spectra, the 2956, 1427, 1302, 1202, 1050, 881, and 744 cm^{-1} absorption peaks can be attributed to $-\text{CH}_3$ absorption, $\text{C}=\text{C}$ stretching, isopropyl, $\text{O}-\text{C}-\text{O}$ stretching, the substituted aromatic, epoxy group, and out-of-plane deformation of the carbonate group, respectively [22]. For the spectra of AE/TGA, no new absorption bands were observed, which suggested that no chemical interaction occurred between AE and TGA.

Three typical characteristic absorption bands for amide were observed at 1660, 1539, and 1234 cm^{-1} and were assigned to $\text{C}=\text{O}$ stretching (amide I), $\text{N}-\text{H}$ bending (amide II), $\text{N}-\text{H}$ in-plane and $\text{C}-\text{N}$ stretching vibration (amide III), respectively [28]. The broad band at 3323 cm^{-1} corresponded to free and bound $\text{N}-\text{H}$ and $\text{O}-\text{H}$ groups, which were the source of intermolecular hydrogen bonding. A plethora of hydrogen bonds can easily form between them and other functional groups of protein molecular to produce mechanical strength [29]. After TGA was added

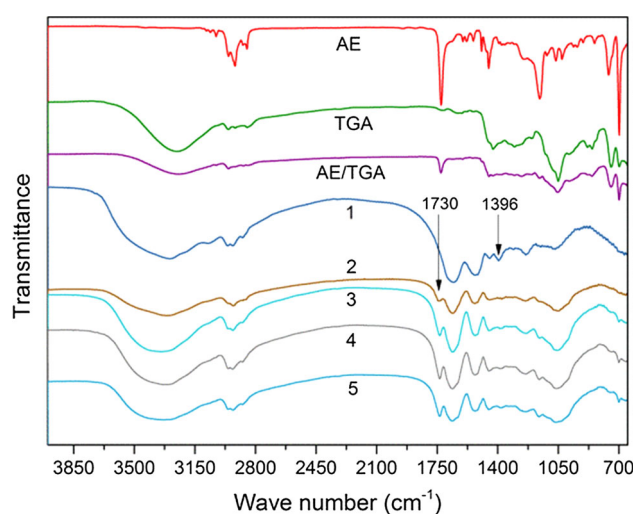


Figure 4 FTIR spectra of the cured AE, TGA, AE/TGA, and adhesive 1 (SM), 2 (SM/TGA), 3 (SM/TGA/2 % AE), 4 (SM/TGA/6 % AE), 5 (SM/TGA/8 % AE).

into SM adhesives, free epoxy groups were not observed in the cured adhesives, which suggested that the TGA was dispersed homogeneously in the adhesive system and adequately participated in the cross-linking reaction. In cured SM/TGA adhesives (adhesive 2, 3, 4, 5), the absorption band at 1396 cm^{-1} was significantly weakened, which suggested that amino group was transformed by the reaction with epoxy group.

Meanwhile, a new peak at 1730 cm^{-1} appeared (adhesive 2), which was related to the carbonyl group of the ester bond and originated from the esterification reaction between epoxy groups and carbonyl groups of soy protein [30]. The cross-linking reaction produced more stable chemical bonds that replaced the weak intermolecular hydrogen bond and formed a cross-linking network in the cured adhesive system, thus improving the water resistance of the adhesive. However, the inherent brittleness of SM adhesive could be aggravated by the cross-linking reaction because the cured TGA (an epoxy-based cross-linker) is a brittle system. Because there was no chemical reaction between AE and TGA, the AE small molecules will permeate into the gap of cross-linked soy protein macromolecular to cure and develop an interpenetrating network (IPN). Through introducing flexible AE into cross-linking network, the IPN will possess compromised toughness and enhanced performance of adhesive and bonded plywood. The schematic diagram of the adhesive cross-linking and interpenetrating network formation is shown in Fig. 5.

XRD analysis

XRD patterns of the cured adhesives are presented in Fig. 6 and their corresponding crystallinity and the mass loss after hydrolyzing are shown in Fig. 7. The XRD pattern of SPAs has two obvious peaks at 2θ of about 9° and 20° , which respectively belong to the α -helix and β -sheet structure of protein molecules [31].

As shown in the two figures, two obvious decreases were observed in peak intensity and crystallinity. The first decrease was induced by TGA cross-linking, and the corresponding crystallinity decreased from 23.74 to 19.37 %. Generally, crystallization is the ordered array of molecules and cross-linking will decrease the crystallinity of the adhesive system [32]. In other words, the decrease in crystallinity confirmed the occurrence of cross-linking reaction

Figure 5 The cross-linking mechanism and interpenetrating network formation of the SPAs.

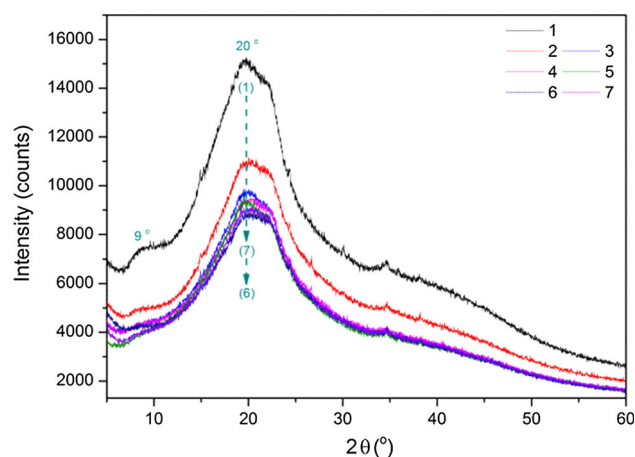
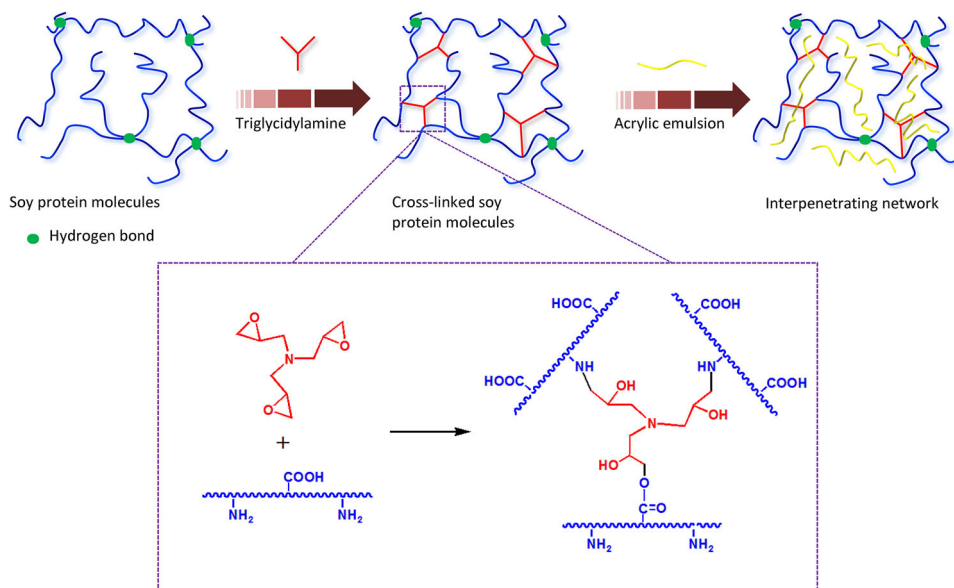


Figure 6 XRD patterns of the cured adhesive 1 (SM), 2 (SM/TGA), 3 (SM/TGA/2 % AE), 4 (SM/TGA/4 % AE), 5 (SM/TGA/6 % AE), 6 (SM/TGA/8 % AE), 7 (SM/TGA/10 % AE).

between TGA and the soy protein molecules as it was observed in FTIR analysis. The second decrease appeared when AE was added, and the crystallinity gradually decreased with AE content increased to 8 % where modified adhesive possessed the lowest crystallinity of 15.89 %. This should be attributed to the formation of IPN in the cured adhesive system. The IPN may break the symmetry of molecular chain and regularity of the arrangement and decrease the crystallization of soy protein molecules. Moreover, the crystallization of AE itself from excess addition increased the crystallinity in SM/TGA/10 % AE adhesive.

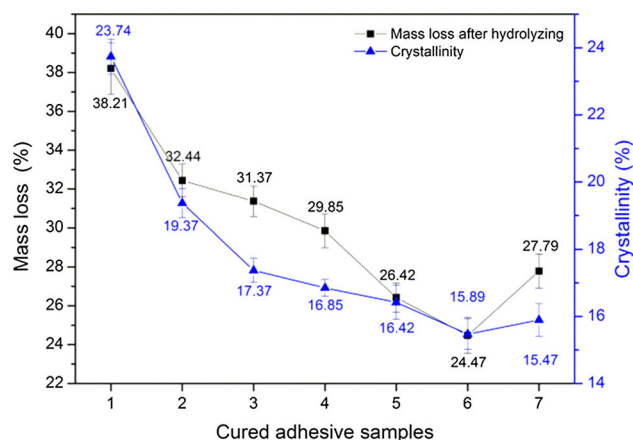


Figure 7 The crystallinity and mass loss after hydrolyzing of the cured adhesive 1 (SM), 2 (SM/TGA), 3 (SM/TGA/2 % AE), 4 (SM/TGA/4 % AE), 5 (SM/TGA/6 % AE), 6 (SM/TGA/8 % AE), 7 (SM/TGA/10 % AE).

As shown in Fig. 7, the mass loss of the cured adhesives after hydrolyzing exhibited the same change tendency. The SM adhesive showed the largest mass loss of 38.21 %, and the TGA reduced it to 32.44 %, which indicated that introduction of 8 % TGA provided an improvement of 15.1 % in the water resistance of SM adhesive. This is because TGA cross-linked the dissoluble molecules of adhesive and elevated the cross-linking density, which can help the adhesive to prevent water intrusion and strengthen the mechanical properties of plywood [20]. After AE was introduced into the TGA/SM adhesive, the water resistance of adhesive was further improved.

When 8 % AE was added, the water resistance was improved by 24.6 % compared with that of SM/TGA adhesive. The improvement probably due to the IPN further increased cross-linking density (the second decrease in crystallinity) and prevented water intake or absorption. However, SM/TGA/10 % AE adhesive conversely showed an increased mass loss, which may be attributable to the hydrolytic sensitivity of emulsifier in AE.

Thermal stability

The thermal degradation process of cured AE, TGA, and their blends are shown in Fig. 8. The pure AE and TGA showed obvious degradation peak at 403 and 244 °C, which also appeared in the blends. Simultaneously, no new degradation peak was observed, indicating that AE did not react with TGA but with physical interpenetration. This verified the results in the FTIR and XRD analysis.

Figure 9 shows the DTG curves of cured different adhesive samples. The thermal degradation of SM adhesive can be divided into three stages [19]. The first (I) stage was the postcuring stage from 120 to 200 °C. In this stage, a further curing reaction occurred between the cross-linker and the soy protein and produced vapor and gases, leading to a mass loss in the adhesive. The second (II) stage was the initial degradation stage from 200 to 280 °C with an obvious peak at about 240 °C. In addition to the decomposition of small molecules and unstable chemical bonds [33], this stage can also be attributed to the

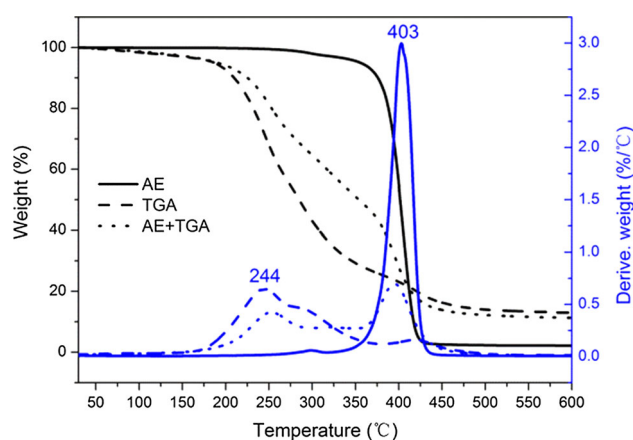


Figure 8 TG and derivative thermogravimetric (DTG) curves of AE, TGA, AE + TGA (50 % AE).

degradation of modifier. The third (III) stage was the skeleton structure degradation stage in the temperature range of 280–370 °C with a peak of about 328 °C. In this stage, the weight loss resulted from the degradation of intermolecular and intramolecular hydrogen bonds, electrostatic bonds, and bond cleavage in soy protein [34]. After incorporating AE, a new degradation stage (IV) in the temperature range of 375–450 °C with a peak at 400 °C was observed, which was attributed to the degradation of the cured AE. Before the first degradation stage (<120 °C), a small mass loss with a peak at about 60 °C resulted from the evaporation of residual moisture. After the fourth degradation stage (>450 °C), soy protein backbone peptide bonds were decomposed to various gases, such as CO, CO₂, NH₃, and H₂S [35]. When AE was introduced to SM/TGA adhesive, the postcuring process at stage I moved to a lower temperature, indicating that AE accelerates the curing of blending adhesive, which may improve the bond strength through a more complete cure. In stage III, TGA incorporating increased the peak temperature from 313 to 328 °C, which suggested that the cross-linked soy protein possessed better thermal stability. It was due to the formation of more stable chemical bonds by the cross-linking reaction between TGA and soy protein molecules. In stage IV, the peak intensity at 400 °C was increased with an increased AE content. The weight loss of SM/TGA/2 % AE to SM/TGA/10 % AE adhesive in stage IV

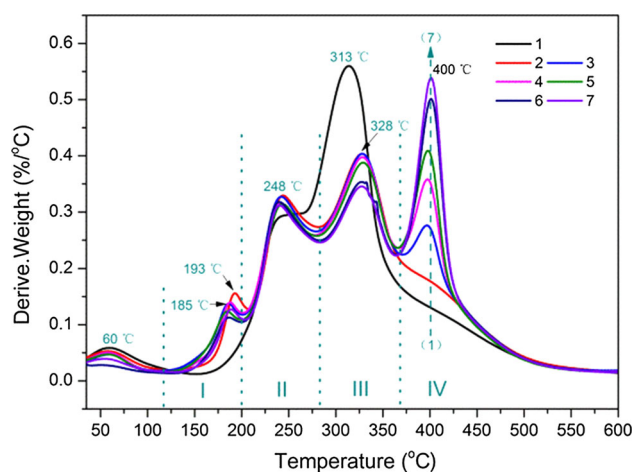


Figure 9 DTG curves of 1 (SM), 2 (SM/TGA), 3 (SM/TGA/2 % AE), 4 (SM/TGA/4 % AE), 5 (SM/TGA/6 % AE), 6 (SM/TGA/8 % AE), 7 (SM/TGA/10 % AE).

was 21.15, 24.32, 25.94, 29.04, and 30.26 %, respectively. This indicated that the SM/TGA/AE adhesives had better thermal stability after forming the IPN.

Toughness evaluation of cured adhesive

Figure 10 shows the toughness of the cured adhesives. As shown in this figure, the neat SM adhesive was a brittle system and exhibited a significant number of small cracks. After cross-linked by TGA, the SM/TGA adhesive became compact, but had larger cracks, which revealed the aggravated brittleness of cured adhesive system. When AE was introduced, cracks disappeared and the surface became homogeneous and more compact than SM/TGA adhesive. Moreover, the homogeneity and compactness increased with increasing AE content. All findings suggested that the inherent brittleness of the SPAs was deteriorated by TGA cross-linking, followed by toughening using flexible AE to form an interpenetrating network.

SEM analysis

The fracture surface micrographs of cured adhesives are shown in Fig. 11. A loose fracture surface with some cracks was observed in the neat SM adhesive, which revealed the inherent brittle and the cohesive failure caused by the evaporation of a large quantity of water. These cracks would provide a channel for moisture attack and caused low water resistance of adhesive [20, 36]. In SM/TGA adhesive, cracks disappeared and the fracture surface became compact. However, a

spiculate block-faulted structure was formed, which suggested that TGA cross-linking increased the cohesion of adhesive and simultaneously embrittled the cured system. This confirms the results discussed above (Figs. 4, 10). When AE was introduced into SM/TGA adhesive, these cracks and spiculate block-faulted structure disappeared and the fracture surface gradually became uniform. In SM/TGA/8 % AE adhesive, the fracture surface became smooth and compact, exhibiting an improved toughness of the cured adhesive. The increase in toughness of system is beneficial to increase the crack propagation energy when the system was loaded, and to improve the mechanical properties of resulting plywood [37]. However, excess AE (10 %) caused a distinguishable two-phase cured structure (7 of Fig. 11), probably due to AE itself curing. All results are in accordance with the observations shown in Figs. 3 and 10.

Shear strength of plywood

Table 1 shows the dry and wet shear strength of the resultant plywood. The bond performance of neat SM adhesive was primarily based on intermolecular hydrogen bond. Because of the low solid content (Fig. 3) and the cohesive failure caused by water evaporation (Figs. 10, 11), the neat SM adhesive respectively exhibited a low dry and wet shear strength of 1.08 and 0.38 MPa. When 8 % TGA was added to the SM adhesive, the dry and wet shear strength increased by 15.7 and 86.8 %, respectively. This significant increase can be attributed to the increased solid content (Fig. 3) and the increased cross-linking density (Fig. 7) is caused by the cross-

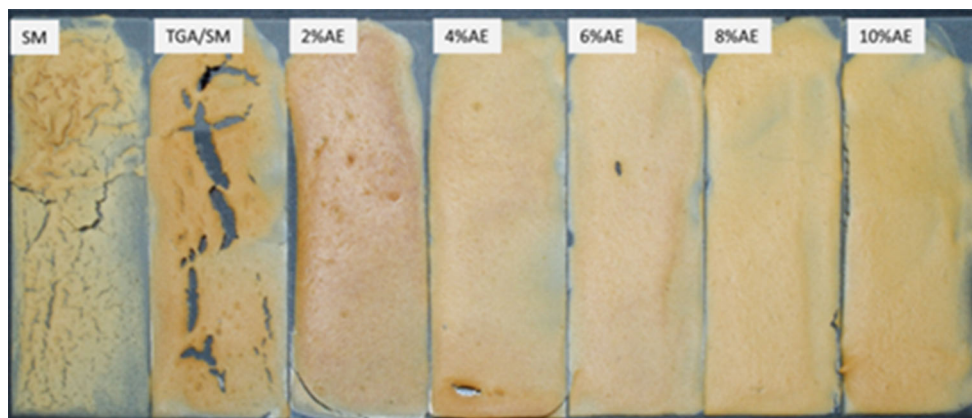


Figure 10 The toughness evaluation of the cured adhesive 1 (SM), 2 (SM/TGA), 3 (SM/TGA/2 % AE), 4 (SM/TGA/4 % AE), 5 (SM/TGA/6 % AE), 6 (SM/TGA/8 % AE), 7 (SM/TGA/10 % AE).

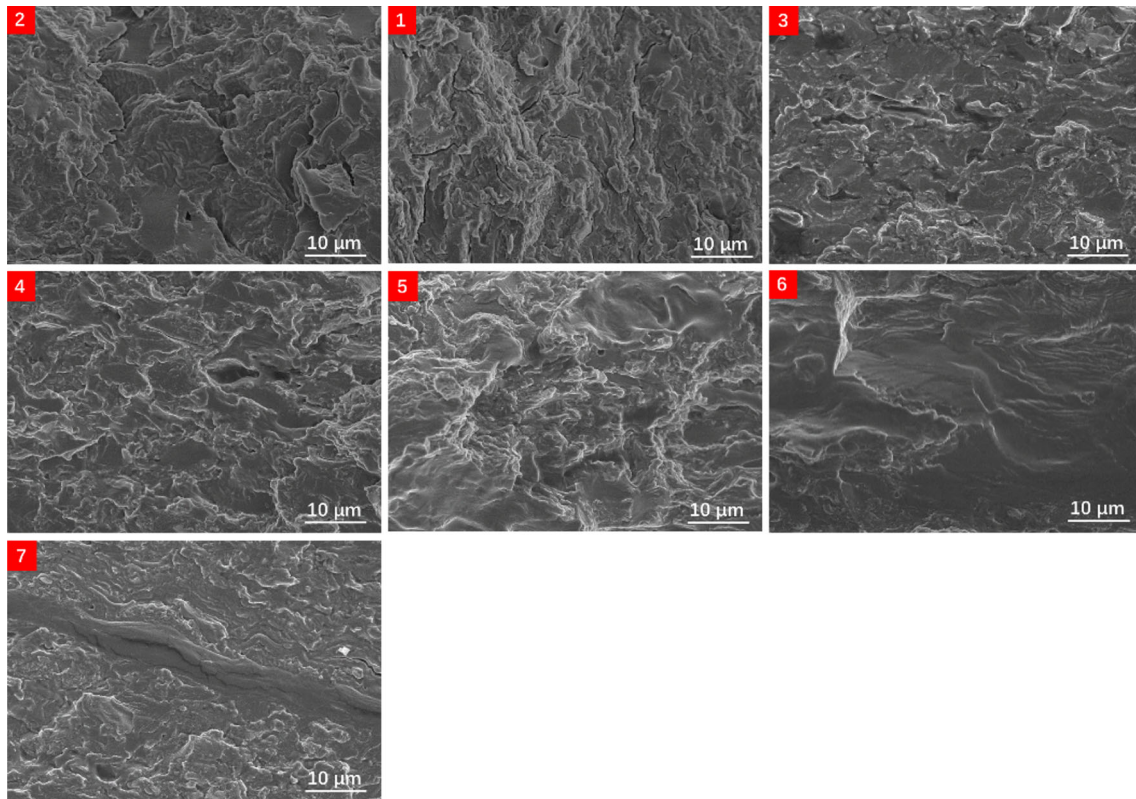


Figure 11 Fracture surface micrographs of the cured adhesive 1 (SM), 2 (SM/TGA), 3 (SM/TGA/2 % AE), 4 (SM/TGA/4 % AE), 5 (SM/TGA/6 % AE), 6 (SM/TGA/8 % AE), 7 (SM/TGA/10 % AE).

Table 1 Dry and wet shear strength of the plywood bonded by adhesive 1 (SM), 2 (SM/TGA), 3 (SM/TGA/2 % AE), 4 (SM/TGA/4 % AE), 5 (SM/TGA/6 % AE), 6 (SM/TGA/8 % AE), 7 (SM/TGA/10 % AE)

Adhesive	1	2	3	4	5	6	7
Dry strength (MPa)	1.08 ± 0.15	1.25 ± 0.09	1.46 ± 0.18	1.68 ± 0.20	1.75 ± 0.11	1.80 ± 0.12	1.82 ± 0.15
Wet strength (MPa)	0.38 ± 0.03	0.71 ± 0.02	0.75 ± 0.06	0.87 ± 0.04	0.95 ± 0.06	1.05 ± 0.03	1.01 ± 0.05

linking reaction between soy protein and the TGA (Fig. 4). Although a considerable increase (15.7 %) was observed, the insufficient dry shear strength (1.25 MPa) indicated the inherent low dry strength of the resultant plywood. This was due to the aggravated inherent brittleness of the SM adhesive after TGA cross-linking (Figs. 10, 11).

The introduction of AE further enhanced the performance of plywood. With the addition of 8 % AE, the dry and wet shear strength of plywood increased by 44.0 and 47.9 % compared with that bonded by SM/TGA adhesive. Improvement in the mechanical properties of plywood may be attributable to the improved toughness using interpenetrating AE network which showed improved water resistance of

adhesive (Fig. 7) and good crack propagation resistance (Fig. 11). In addition, the accelerated curing in hot-pressing process (Fig. 9) may be another contributor to improved mechanical properties. However, plenty of emulsifier was brought in the adhesive system and caused a decrease in water resistance of adhesive (Fig. 7). This is the reason why 10 % AE increased the dry shear strength but sacrificed the wet shear strength of plywood.

Conclusions

The following conclusions can be drawn from the results obtained in this report:

- (1) Addition of 8 % TGA increased the solid content of the adhesive to 30.44 %, which was further increased to 35.92 % as 8 % AE addition. The increased solid content reduced the cohesive failure of cured adhesive by limiting the water evaporation.
- (2) Use of 8 % TGA in SM adhesive improved the water resistance of the adhesive by 15.1 % and the wet shear strength of resultant plywood by 86.8 % because of the formation of a cross-linking network through the reaction between TGA and the soy protein molecules. However, TGA cross-linking also increased the inherent brittleness of SM adhesive and resulted in low dry strength issue of plywood.
- (3) Using AE improved the toughness of cured adhesive, which increased the crack propagation energy and enhanced the performance of adhesive and plywood.
- (4) The incorporation of 8 % AE further increased the water resistance of SM/TGA adhesive by 24.6 %, the wet shear strength of plywood by 47.9 %, and the dry shear strength of plywood by 44.0 %, respectively because of the formation of an interpenetrating network.
- (5) Adding flexible modifier to toughen the SPAs adhesive can effectively improve the water resistance of adhesive and solve the low dry strength issue of resultant composites.

Acknowledgements

The authors are grateful for financial support from Beijing Natural Science Foundation (2151003) and the Special Fund for Forestry Research in the Public Interest (201404501).

References

- [1] Pizzi A (2013) Bioadhesives for wood and fibres: a critical review. *Rev Adhes Adhes* 1:88–113. doi:[10.7569/RAA.2013.097303](https://doi.org/10.7569/RAA.2013.097303)
- [2] Pizzi A (2006) Recent developments in eco-efficient bio-based adhesives for wood bonding: opportunities and issues. *J Adhes Sci Technol* 20:829–846. doi:[10.1163/156856106777638635](https://doi.org/10.1163/156856106777638635)
- [3] Nordqvist P, Nordgren N, Khabbaz F, Malmström E (2013) Plant proteins as wood adhesives: bonding performance at the macro- and nanoscale. *Ind Crop Prod* 44:246–252. doi:[10.1016/j.indcrop.2012.11.021](https://doi.org/10.1016/j.indcrop.2012.11.021)
- [4] Acosta E (2007) Protein bioadhesives. *Inform Cham* 18:56
- [5] Cheng HN, Ford C, Dowd MK, He Z (2016) Soy and cottonseed protein blends as wood adhesives. *Ind Crop Prod* 85:324–330. doi:[10.1016/j.indcrop.2015.12.024](https://doi.org/10.1016/j.indcrop.2015.12.024)
- [6] Khosravi S, Nordqvist P, Khabbaz F, Öhman C, Bjurhager I, Johansson M (2015) Wetting and film formation of wheat gluten dispersions applied to wood substrates as particle board adhesives. *Eur Polym J* 67:476–482. doi:[10.1016/j.eurpolymj.2014.11.034](https://doi.org/10.1016/j.eurpolymj.2014.11.034)
- [7] Li N, Wang Y, Tilley M, Bean SR, Wu X, Sun XS, Wang D (2011) Adhesive performance of sorghum protein extracted from sorghum DDGS and flour. *J Polym Environ* 19:755–765. doi:[10.1007/s10924-011-0305-5](https://doi.org/10.1007/s10924-011-0305-5)
- [8] Li J, Li X, Li J, Gao Q (2015) Investigating the use of peanut meal: a potential new resource for wood adhesives. *RSC Adv* 5:80136–80141
- [9] Ghosh Dastidar T, Netravali AN (2013) A soy flour based thermoset resin without the use of any external crosslinker. *Green Chem* 15:3243–3251. doi:[10.1039/C3GC40887F](https://doi.org/10.1039/C3GC40887F)
- [10] Sun XS (2011) Soy protein polymers and adhesion properties. *J Biobased Mater Bioenergy* 5:409–432. doi:[10.1166/jbmb.2011.1183](https://doi.org/10.1166/jbmb.2011.1183)
- [11] Frihart CR, Birkeland MJ (2014) Soy properties and soy wood adhesives. In: Brentin RP (ed) *Soy-Based Chemicals and Materials*. Oxford University Press, Washington, DC, pp 167–192
- [12] Nordqvist P, Khabbaz F, Malmström E (2010) Comparing bond strength and water resistance of alkali-modified soy protein isolate and wheat gluten adhesives. *Int J Adhes Adhes* 30:72–79. doi:[10.1016/j.ijadhadh.2009.09.002](https://doi.org/10.1016/j.ijadhadh.2009.09.002)
- [13] Huang W, Sun X (2000) Adhesive properties of soy proteins modified by urea and guanidine hydrochloride. *J Am Oil Chem Soc* 77:101–104. doi:[10.1007/s11746-000-0016-6](https://doi.org/10.1007/s11746-000-0016-6)
- [14] Huang W, Sun X (2000) Adhesive properties of soy proteins modified by sodium dodecyl sulfate and sodium dodecylbenzene sulfonate. *J Am Oil Chem Soc* 77:705–708. doi:[10.1007/s11746-000-0113-6](https://doi.org/10.1007/s11746-000-0113-6)
- [15] Wang Y, Mo X, Sun XS, Wang D (2007) Soy protein adhesion enhanced by glutaraldehyde crosslink. *J Appl Polym Sci* 104:130–136. doi:[10.1002/app.24675View/savecitation](https://doi.org/10.1002/app.24675View/savecitation)
- [16] Liu Y, Li K (2007) Development and characterization of adhesives from soy protein for bonding wood. *Int J Adhes Adhes* 27:59–67. doi:[10.1016/j.ijadhadh.2005.12.004](https://doi.org/10.1016/j.ijadhadh.2005.12.004)
- [17] Gao Q, Qin Z, Li C, Zhang S, Li J (2013) Preparation of wood adhesives based on soybean meal modified with PEGDA as a crosslinker and viscosity reducer. *BioResources* 8:5380–5391

- [18] Li H, Li C, Gao Q, Zhang S, Li J (2014) Properties of soybean-flour-based adhesives enhanced by attapulgite and glycerol polyglycidyl ether. *Ind Crop Prod* 59:35–40. doi:[10.1016/j.indcrop.2014.04.041](https://doi.org/10.1016/j.indcrop.2014.04.041)
- [19] Li J, Luo J, Li X, Yi Z, Gao Q, Li J (2015) Soybean meal-based wood adhesive enhanced by ethylene glycol diglycidyl ether and diethylenetriamine. *Ind Crop Prod* 74:613–618. doi:[10.1016/j.indcrop.2015.05.066](https://doi.org/10.1016/j.indcrop.2015.05.066)
- [20] Luo J, Li C, Li X, Luo J, Gao Q, Li J (2015) A new soybean meal-based bioadhesive enhanced with 5,5-dimethyl hydantoin polyepoxide for the improved water resistance of plywood. *RSC Adv* 5:62957–62965. doi:[10.1039/C5RA05037E](https://doi.org/10.1039/C5RA05037E)
- [21] Wang RM, Wang JF, Wang XW, He YF, Zhu YF, Jiang ML (2011) Preparation of acrylate-based copolymer emulsion and its humidity controlling mechanism in interior wall coatings. *Prog Org Coat* 71:369–375. doi:[10.1016/j.porgcoat.2011.04.007](https://doi.org/10.1016/j.porgcoat.2011.04.007)
- [22] Connolly JM, Alferiev I, Eidelman N, Sacks M, Palmatory E, Kronsteiner A, DeFelice S, Xu J, Ohri R, Narula N, Vyavahare N, Levy RJ, Clark-Gruel JN (2005) Triglycidylamine crosslinking of porcine aortic valve cusps or bovine pericardium results in improved biocompatibility, biomechanics, and calcification resistance: chemical and biological mechanisms. *Am J Pathol* 166:1–13. doi:[10.1016/S0002-9440\(10\)62227-4](https://doi.org/10.1016/S0002-9440(10)62227-4)
- [23] GB/T 14074, (2006) Standardization Administration of the People's Republic of China, Beijing
- [24] GB/T 17657, (2013) Standardization Administration of the People's Republic of China, Beijing
- [25] Poletto M, Zattera AJ, Forte MMC, Santana RMC (2012) Thermal decomposition of wood: influence of wood components and cellulose crystallite size. *Bioresource Technol* 109:148–153. doi:[10.1016/j.biortech.2011.11.122](https://doi.org/10.1016/j.biortech.2011.11.122)
- [26] Kamke FA, Lee JN (2007) Adhesive penetration in wood—a review. *Wood Fiber Sci* 39:205–220
- [27] Liu Y, Li K (2002) Chemical modification of soy protein for wood adhesives. *Macromol Rapid Comm* 23:739–742. doi:[10.1002/1521-3927\(20020901\)23:13<739:AID-MARC739>3.0.CO;2-0](https://doi.org/10.1002/1521-3927(20020901)23:13<739:AID-MARC739>3.0.CO;2-0)
- [28] Gerrard JA (2002) Protein–protein crosslinking in food: methods, consequences, applications. *Trends Food Sci Tech* 13:391–399. doi:[10.1016/S0924-2244\(02\)00257-1](https://doi.org/10.1016/S0924-2244(02)00257-1)
- [29] Karnnet S, Potiyaraj P, Pimpan V (2005) Preparation and properties of biodegradable stearic acid-modified gelatin films. *Polym Degrad Stabil* 90:106–110. doi:[10.1016/j.polydegradstab.2005.02.016](https://doi.org/10.1016/j.polydegradstab.2005.02.016)
- [30] Mekonnen TH (2014) Valorization of waste protein biomass for bio-based plastics, composites and adhesives development. PhD Dissertation, University of Alberta
- [31] Chen J, Chen X, Zhu Q, Chen F, Zhao X, Ao Q (2013) Determination of the domain structure of the 7S and 11S globulins from soy proteins by XRD and FTIR. *J Sci Food Agr* 93:1687–1691. doi:[10.1002/jsfa.5950](https://doi.org/10.1002/jsfa.5950)
- [32] Colby R, Rubinstein M (2003) *Polymer physics*. Oxford University Press, New York
- [33] Kumar R, Choudhary V, Mishra S, Varma IK (2004) Enzymatically-modified soy protein part 2: adhesion behaviour. *J Adhes Sci Technol* 18:261–273. doi:[10.1163/156856104772759458](https://doi.org/10.1163/156856104772759458)
- [34] Qin Z, Gao Q, Zhang S, Li J (2013) Glycidyl methacrylate grafted onto enzyme-treated soybean meal adhesive with improved wet shear strength. *BioResources* 8:5369–5379
- [35] Qi G, Sun X (2011) Soy protein adhesive blends with synthetic latex on wood veneer. *J Am Oil Chem Soc* 88:271–281. doi:[10.1007/s11746-010-1666-y](https://doi.org/10.1007/s11746-010-1666-y)
- [36] Zhang Y, Zhu W, Lu Y, Gao Z, Gu J (2014) Nano-scale blocking mechanism of MMT and its effects on the properties of polyisocyanate-modified soybean protein adhesive. *Ind Crop Prod* 57:35–42. doi:[10.1016/j.indcrop.2014.03.027](https://doi.org/10.1016/j.indcrop.2014.03.027)
- [37] Gao Z, Zhang Y, Fang B, Zhang L, Shi J (2015) The effects of thermal-acid treatment and crosslinking on the water resistance of soybean protein. *Ind Crop Prod* 74:122–131. doi:[10.1016/j.indcrop.2015.04.026](https://doi.org/10.1016/j.indcrop.2015.04.026)